Journal of the Korean Ceramic Society
Vol. 41, No. 1, pp. 19~23, 2004.

Indentation Damage of Porous Alumina Ceramics

Jang-Hoon Ha,† Chul-Seung Lee, Jong Ho Kim, and Do Kyung Kim

Department of Materials Science and Engineering, Korea Advanced Institute of Science and Technology, Daejeon 305-701, Korea

(Received October 17, 2003; Accepted December 10, 2003)

ABSTRACT

The Hertzian indentation contact damage behavior of porous alumina with controlled pore shape was investigated by experiments. Porous alumina ceramics containing well-defined pore shape, size and distribution were prepared by incorporation of fugitive spherical starch. Porous alumina with isolated pore structure was prepared with porosity range up to 30%. The indentation stress-strain curves of porous alumina were constructed. Elastic modulus and yield stress can be obtained from the stress-strain relationship. Impulse excitation method for the measurement of elastic modulus was also conducted as well as Hertzian indentation and was confirmed as a useful tool to evaluate the elasticity of highly porous ceramics. Elastic modulus of the inter-connected pore structure is more sensitive to porosity than that of the isolated pore structure. When the specimen had isolated pore structure, higher yield point was obtained than it had inter-connected pore structure. This study proposed that the elastic modulus of porous ceramics is strongly related to not only porosity, but also the structure of pore.

Key words : Elastic modulus, Porous ceramics, Hertzian indentation, Isolated pore, Inter-connected pore

1. Introduction

Ceramic materials have excellent properties such as high wear resistance, hardness, thermal shock resistance and corrosion resistance. Porous ceramics have been investigated through past two decades in various fields such as environmental ceramics (diesel particulate filter and membrane), bio-ceramics (implant and artificial bone), and structural ceramics (thermal insulation, sound absorption, and lightweight usage). When pores or flaws are contained in materials, they influence the elastic and mechanical properties of the material.[1] The presence of small pores results in a sharp decrease in strength and elastic modulus.[2] This has an important meaning because elastic modulus is a fundamental property of structural materials, and in ceramic materials low Youngs modulus is a barrier to structural application with low strength. The porous materials have to keep structural reliability for practical use. Before the application, the morphology-elasticity relationship has to be presented. The elastic properties of porous ceramics depend on the pore geometry as well as the value of porosity. To predict properties or properly interpret the properties of porous ceramics, it is needed to have an accurate method of relating elastic properties to porosity and microstructure. Many researchers have studied the effect of pore structure, shape, and size.[3-8] Theoretical and experimental work has been done and numerous relationships have been put forward. Most relationship shows the variation of elastic constant, usually elastic modulus.

In this study, alumina was selected as a model porous ceramics to reveal the effect of pore structure on the contact damage. Fugitive spherical starch was also used to fabricate porous alumina with selected porosity. Starch was profitable because spherical pore was more convenient to study the effect of pore structure, shape, and size than irregular pore that was usually induced by naphthalene or carbon. The work was concerned with the fabrication of alumina that had isolated pore structure. Hertzian indentation technique[9-11] was used to investigate the effect of contact damage of porous ceramics. Contact damage response of porous alumina was observed by using the bonded-interface specimen and elastic modulus was evaluated using impulse excitation method as well as Hertzian indentation. Relative density as a function of the fugitive spherical starch has been measured. Cross-sections of the materials have been observed using SEM.

2. Experimental Procedure

2.1. Specimen Preparation

Starting powders were prepared comprising a mixture of alumina (AKP-50, Sumitomo, Japan) and potato-starch, (Aldrich, USA) in ethanol. The slurries were ball-milled with zirconia balls for 5 h and then oven-dried at 60°C for 24 h. Green bodies were formed rectangle specimens (length 30-32 mm, width 5-6 mm, thickness 2-3 mm) and prepared by Cold-Isostatic Pressing (CIP) at 200 MPa and then

†Corresponding author : Jang-Hoon Ha
E-mail : hjhoon@kaist.ac.kr
Tel : +82-42-869-4151 Fax : +82-42-869-3310

sintered at 1600°C for 5 h using box furnace in air atmosphere. Processing method was removal of fugitive material added to the body. In this study, alumina was the body and starch was fugitive material, respectively. In sintering process, starch burn-out occurred during sintering. When starch burned out, heating rate was 50°C/h to prevent evaporated starch combustion gas from remaining in matrix. Then, well-defined pores were formed in alumina matrix. Target porosity range was planned to be less than 30% to avoid pore clustering that can bring about additional effects. To prepare the specimens for Scanning Electron Microscope (SEM) observation, standard polishing techniques were employed. The specimens were ground using 20 μm diamond grinding-disc and the surface perpendicular to thickness was polished to a 1ìm finish. Densities were measured by Archimedes method. Porosities were calculated from the bulk density and the theoretical density.

2.2. Hertzian Indentation

Fig. 1 shows schematic configuration of Hertzian contact of sphere on the specimen. Consider indentation on a ceramic surface by a sphere of radius r_i and normal loading P, over a contact radius a. Hertzian indentation contains a large component of hydrostatic compression, considerable shear, and modest tension. For general purposes, it is useful to define an effective radius by $1/r = 1/r_c + 1/r_i$ with subscripts c and i referring to ceramic and indenter materials, respectively. These definitions are simple but useful for other configurations to predict response of surface contact damage of complex geometries. For elastic Hertzian contact behavior, the relationship between the contact radius and the indentation load is

$$a^3 = \frac{3PR}{4E^*} \tag{1}$$

where $1/E = (1-\upsilon_c^2)/E_c + (1-\upsilon_c^2)/E_i$. The radius of contact is a, R is the radius of the indenter, and P is the applied load. Elastic modulus is E and $\tilde{o}$ is the Poissons ratio. This relation can be handled to show an elastic indentation stress-strain relation.

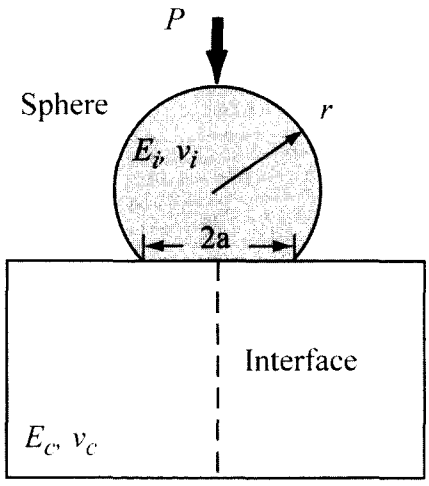

Fig. 1. Schematic configuration of Hertzian contact of sphere on the bonded-interface specimen.

$$P_m = \left[\frac{4E^*}{3\pi}\right]\frac{a}{R} \tag{2}$$

where $P_m = P/\pi a^2$ is the mean indentation stress and a/R is a relative indentation strain. Elastic modulus is obtained by using the slope of the plot of indentation stress versus a/R.

In relation to the uniaxial compression yield stress Y,

$$p_y = P_Y/\pi a^2 = 1.1Y \tag{3}$$

In previous equation, p_Y is the mean contact pressure at yield stress point and measurement of p_Y affords a simple means for determining the yield stress Y.[9] The critical contact load, P_Y is determined at the transition point when the indentation stress-strain relations deviate from elastic to quasi-plastic response.

The porous alumina was subjected to top-surface contact loading from tungsten carbide indenting spheres (radius 1.98 mm, 3.57 mm, 3.96 mm, and 4.76 mm) mounted into the crosshead of a mechanical loading machine (Model 4400R, Instron Corp., Canton, MA, USA). The crosshead was lowered until the sphere contacted the top surface of the specimen. The load P was then increased at a constant load rate of 10 Ns^{-1} to a specified peak value. Several tests were performed on every specimen over a load range of 1000-2500 N.

A bonded-interface technique was used to examine the subsurface contact damage. Two polished-blocks were joined by glass glue. The bonded specimens were separated and the surfaces cleaned with acetone. The specimens were gold-coated and viewed in an optical microscope using Nomarski interference to observe macroscopic damage patterns.

2.3. Impulse Excitation Method

Elastic modulus measurement technique was impulse excitation of vibration method (ASTM E1876-1).[12] In general, pulse-echo method is widely used. For highly porous materials, impulse excitation method is more convenient and can be used on small-sized specimens of porous materials. Elastic modulus can be calculated directly using Eq. (4).

$$E = 0.9465(mf_f^2/b)(L^3/t^3)T_1 \tag{4}$$

Where E = Young's modulus, (Pa), m = mass of the bar, (g), b = width of the bar, (mm), L = length of the bar, (mm), t = thickness of the bar, (mm), f_f = fundamental resonant frequency of bar in flexure, (Hz), and T_1 = correction factor for fundamental flexural mode to account for finite thickness of bar, υ = Poisson's ratio, etc. Fig. 2 shows experimental set-up for elastic modulus by impulse excitation method. The resonant frequencies were measured using oscilloscope (Tektronix TDS210 w/FFT module, USA) with non-contact transducer (Cirrus ZE : 901 CRL L3M Preamplifier, USA). Elastic modulus was obtained by impulse excitation ahead

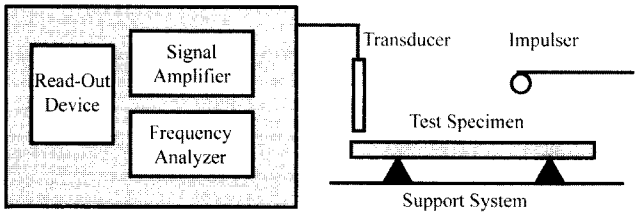

Fig. 2. Experimental set-up for elastic modulus by impulse excitation method.

of Hertzian indentation because impulse excitation was non-destructive test.

3. Results and Discussion

3.1. Microstructure and Porosity

The density and porosity of sintered samples were shown in Fig. 3. Porosity was controlled as a function of the amount of fugitives. As the amount of fugitives increased from 0% to 10%, the porosity increased linearly from 3.8% to 21.3%. Fig. 4 shows polished surface image of alumina with isolated pore structure. SEM images show spherical pores surrounded by a dense alumina matrix. It was observed that spherical pores had the same size as that of starch particles in alumina matrix. As can be observed in Fig. 4, inter-connectivity between pores increased with increasing porosity. Well-defined isolated pores were fabricated up to 30% porosity successfully.

To compare this experiment with inter-connected pore structure, reference data was used. Previous researcher [13] fabricated porous alumina with inter-connected pore structure by sintering of alumina at different temperature and

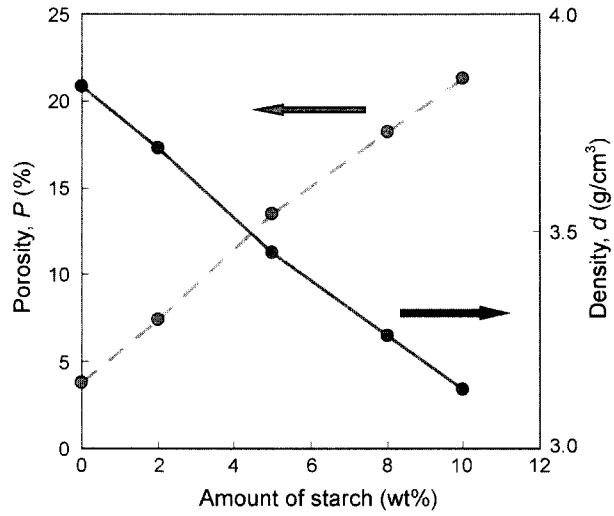

Fig. 3. The density and porosity of sintered alumina.

time. The results showed that increasing porosity induces a transition from an essentially brittle to a quasi-plastic response in the damage mode.

3.2. Hertzian Indentation

This experiment illustrates how the porosity-change in the isolated pore structure affects macroscopic deformation. It can be seen that the damage has the Hertzian cone fracture with ring crack at a load of 1000 N in Fig. 5. At low porosity, the slight damage was observed within semi-spherical region below the contact area. When porosity increased, the residual surface depression and the severity of damage were clearly enhanced. At high porosity (>20%),

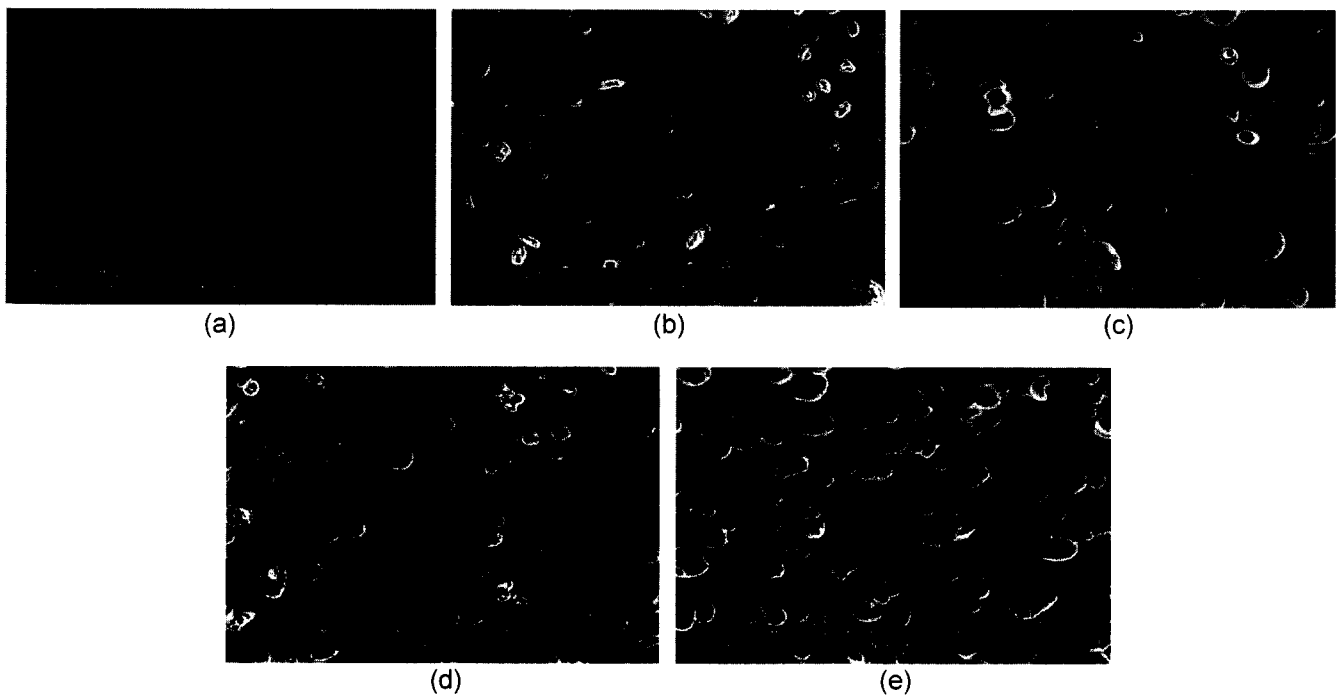

Fig. 4. SEM images of the polished specimens with porosity (a) 3.8%, (b) 7.4%, (c) 13.5%, (d) 18.4%, and (e) 21.3%.

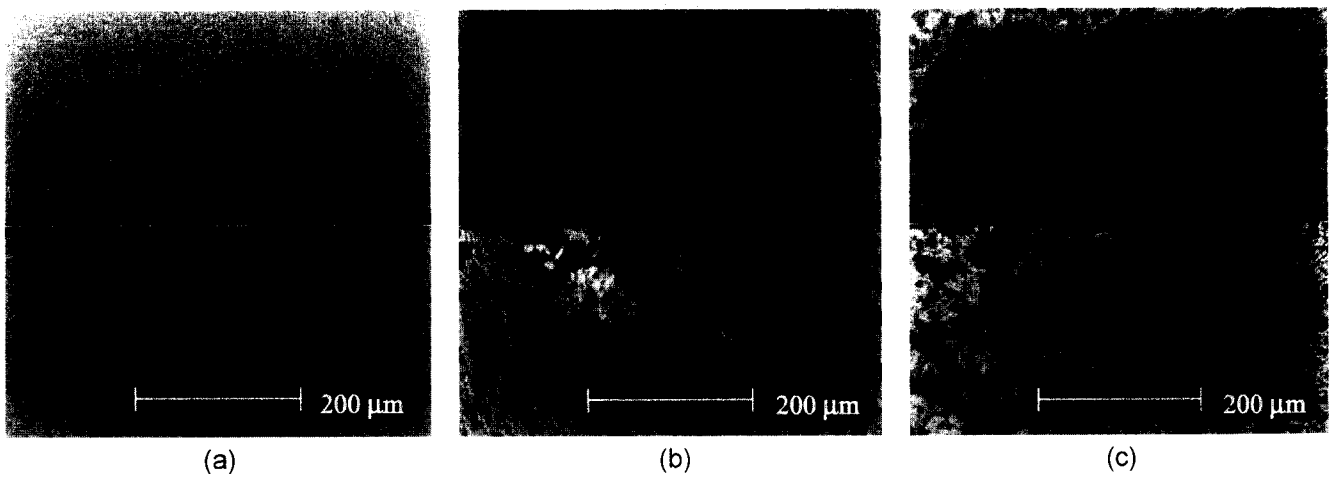

Fig. 5. Optical micrographs of Hertzian indentation sites at a load P=1000 N, comparing damage of porous alumina with porosity (a) 3.8%, (b) 13.5%, and (c) 21.3%.

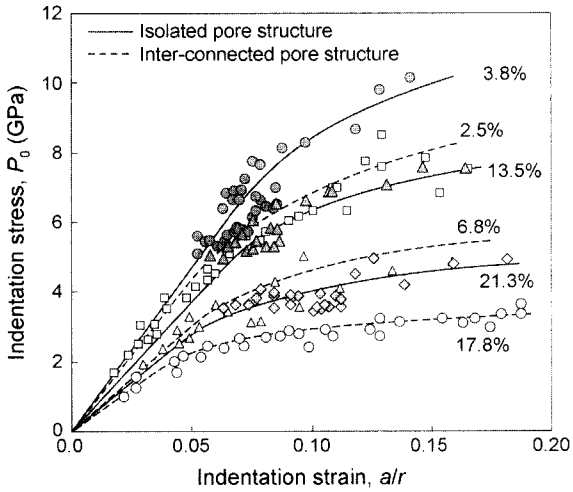

Fig. 6. Indentation stress-strain curve for porous alumina of indicated porosities.

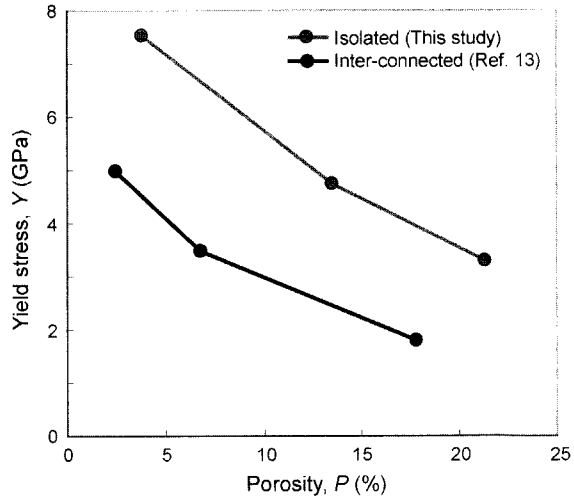

Fig. 7. The plot of yield stress vs. porosity of specimens with reference data.

the damage was significantly enhanced and departed from spherical region. The deviation from elastic response increased and it had quasi-plasticity. Fig. 5(b) and (c) show quasi-plastic behavior at a load of 1000 N and quasi-plasticity became dominant as the microstructure had more inter-connected pores.

Fig. 6 shows the indentation stress-strain curve for porous alumina of indicated porosities. Data were reproduced from this study and reference data.[13] In comparison of this experiment with porous alumina with inter-connected pore structure, the specimens of this study in Fig. 6 had higher porosities and higher elastic modulus. For example, in this study, the specimen with 3.8% porosity had a stiff slope of elastic modulus than the inter-connected pore structure specimen with 2.5% porosity. It was due to the fact that the specimen had isolated pore structure and reference specimen had inter-connected pore structure. Fig. 7 shows the comparison of yield stress between this study and reference data. In general, when porosity was higher, lower yield stress was obtained. When the specimen had isolated pore structure, higher yield point was obtained than it had inter-connected pore structure.

Elastic modulus and yield stress of interconnected pore structure were more sensitive to porosity than those of isolated one. It was due to the fact that inter-connected pore structure had minimum contact area between particles and only necks were formed between particles. The different pore structure induced elastic modulus and yield stress difference at the same porosity. In Figs. 6 and 7, the relationship between pore structure and elastic properties was qualitatively demonstrated. This study proposed that the elastic property degradation was strongly related to not only porosity, but also pore structure.

3.3. Elastic Modulus

Elastic modulus can be predicted with analytic solution and empirical equation. Several works were done to reveal porosity-property relations previously.[14,15]

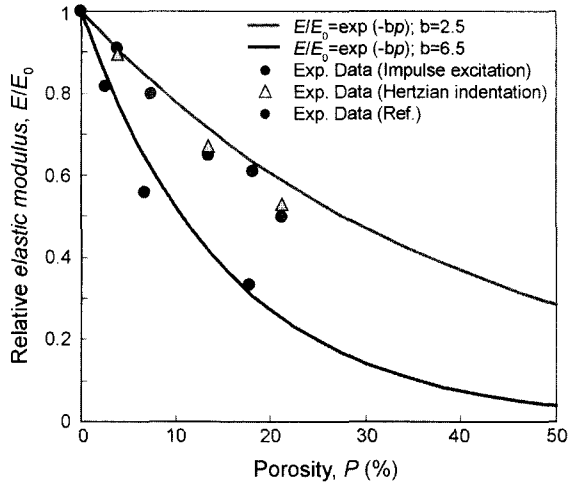

Fig. 8. Elastic modulus obtained by Hertzian indentation and impulse excitation method as a function of porosity with reference data.

$$E = E_0 \exp(-bp) \tag{5}$$

The general form of elastic modulus-porosity correlation is presented as a simple empirical eq. (5).[16] E_0 is zero-porosity elastic modulus, P is the volume fraction of porosity and b is an empirical constant. Spriggs[17] showed that the constant b was 2.73 for slip casting and sintering; 4.08~4.35 for hot pressing; 3.44~3.55 for cold pressing and sintering in empirical background. In general, b value was calculated 6.5 for isolated pore structure and 2.5 for inter-connected pore structure in analytic background by Rice.[8] Theoretically predicted normalized elastic modulus was compared as a function of porosity with experimental data and reference data. Upper line which represents the isolated pore structure was matched well with experiment and lower line which represents the inter-connected pore structure with the specimen had inter-connected pore structure.

Elastic modulus that obtained by Hertzian contact was confirmed by impulse excitation method.

Fig. 8 shows elastic modulus obtained by Hertzian indentation and impulse excitation method as a function of porosity with reference data. Elastic modulus obtained by Hertzian indentation showed slight difference with impulse excitation method. It was tolerable measurement error when indentation area was measured by optical microscope.

4. Conclusion

Porous alumina with isolated pore structure was prepared with wide range of porosity using fugitive spherical starch successfully. From a standpoint of pore structure, elastic modulus and yield stress of inter-connected pore structure were more sensitive to porosity than those of isolated pore structure. It has been shown that isolated pore structure of porous ceramics has more resistance to contact damage. Hertzian indentation could be used to measure the elastic modulus and to reveal the contact damage of porous ceramics. Elastic modulus and yield stress were strongly related to not only porosity, but also the structure of pore.

Acknowledgment

This work is supported by Center for Advanced Materials Processing (CAMP) of the 21st Century Frontier R & D program funded by Korean Ministry of Science and Technology.

REFERENCES

1. R. L. Coble and W. D. Kingery, "Effect of Porosity on Physical Properties of Alumina," *J. Am. Ceram. Soc.*, **39** [11] 377-85 (1956).
2. Z. Hashin, "The Elastic Moduli of Heterogeneous Materials," *J. Appl. Mech.*, **29** [1] 143-50 (1962).
3. N. Ramakrishnan and V. S. Arunachalam, "Effective Elastic Moduli of Ceramic Materials," *J. Am. Ceram. Soc.*, **76** [10] 2745-52 (1993).
4. J. Y. Yun, H. D. Kim, and C. H. Park, "Fabrication of Double-layered Porous Materials," *J. Kor. Ceram. Soc.*, **39** [10] 919-27 (2002).
5. A. R. Boccaccini and Z. Fan, "A New Approach for the Young's Modulus-porosity Correlation of Ceramic Materials," *Ceram. Int.*, **23** 239-45 (1997).
6. A. P. Roberts and E. J. Garboczi, "Elastic Moduli of Model Random Three-dimensional Closed-cell Cellular Solids," *Acta Mater.*, 189-97 (2001).
7. A. P. Roberts and E. J. Garboczi, "Elastic Properties of Model Random Three-dimensional Open-cell Solids," *J. Mech. Phys. Solids*, **50** 33-55 (2002).
8. R. W. Rice, "Porosity of Ceramics," *Marcel Dekker, Inc.*, New York, p. 20 (1997).
9. B. R. Lawn, "Indentation of Ceramics with Spheres : A Century after Hertz," *J. Am. Ceram. Soc.*, **81** [8] 1977-94 (1998).
10. J. She, J. F. Yang, Y. Beppu, and T. Ohji, "Hertzian Contact Damage in a Highly Porous Silicon Nitride Ceramic," *J. Eur. Ceram. Soc.*, **23** 1193-97 (2003).
11. K. S. Lee, D. K. Kim, S. K. Woo, and M. H. Han, "Strength Degradation from Contact Fatigue in Self-toughened Glass-ceramics," *J. Kor. Ceram. Soc.*, **7** [2] 63-9 (2001).
12. "Standard Test Method For Dynamic Young's Modulus, Shear Modulus and Poisson's Ratio by Impulse Excitation of Vibration" *ASTM*, E1876-1.
13. B. A. Latella, B. H. O'Connor, N. P. Padture, and B. R. Lawn, "Hertzian Contact Damage in Porous Alumina Ceramics," *J. Am. Ceram. Soc.*, **80** [4] 1027-31 (1997).
14. R. W. Rice, "Evaluation and Extension of Physical Property-porosity Models Based on Minimum Solid Area," *J. Mater. Sci.*, **31** 102-18 (1996).
15. E. A. Dean and J. A. Lopez, "Empirical Dependence of Elastic Moduli on Porosity for Ceramic Materials," *J. Am. Ceram. Soc.*, **60** [7-8] 345-49 (1977).
16. F. P. Knudsen, "Effect of Porosity on Young's Modulus of Alumina," *J. Am. Ceram. Soc.*, **45** [2] 94-5 (1962).
17. R. M. Spriggs, "Effect of Open and Closed Pores on Elastic Moduli of Polycrystalline Alumina," *J. Am. Ceram. Soc.*, **45** [9] 454 (1962).